PHOTOMETRY ANI) SURFACE STRUCTURE OF THE ICY GALILEAN SATELLITES

Bonnie J. Buratti
Jet Propulsion Laboratory
California Institute of Technology
4800 Oak Grove Dr. 183-501
Pasadena, CA 91109
ph. (818)354-7427
FAX (818)354-0966
buratti@jplpds.jpl.nasa.gov

Submitted to

Journal of Geophysical Research (Planets)

Special issue on Icy Galilean Satellites
Based on an invited review talk presented
at the Icy Galilean Satellite Conference
San Juan Capistrano, Feb. 1-3, 1994

ABSTRACT

Observations of the icy Galilean satellites from both spacecraft and groundbased telescopes have been fit to radiative transfer models describing the surfaces in terms of their roughness, compaction state, and single particle phase function and albedo. The microscopically rough nature of Ganymede and Callisto is similar to the Moon's, while Europa is significantly smoother. The sharply peaked opposition surge on Europa may be due to an extremely uncompacted upper regolith. However, if the peak is attributed to coherent backscatter, its surface may be the most compacted of the Galilean satellites. The compaction state of Callisto is similar to that of the Moon, while Ganymede's surface is more compacted. Callisto and possibly Europa exhibit textural differences in their leading and trailing hemispheres. This dichotomy is due to enhanced erosion by meteorites on the leading side.

I. INTRODUCTION

Photometry is the quantitative measurement of reflected or emitted light. During the past 15 years, photometry of planetary surfaces has expanded as a field of study because of advances in radiative transfer theory and because of the acquisition of radiometrically calibrated observations from spacecraft. The classical study on radiative transfer by Chandrasekhar (1960) has been extended to planetary surfaces of arbitrary albedo (Hapke, 1981, 1984, 1986; Lumme and Bowell, 1981; Goguen, 1981), and to the radiative properties of optically thin atmospheres overlying planetary surfaces (Arvidson et al., 1989; Hillier et al., 1990). By fitting these radiative transfer models to both spacecraft measurements and groundbased observations, investigators have been able to understand the surface properties of a wide variety of celestial bodies, including the Galilean satellites (Burst-ti, 1985, 1991; Helfenstein, 1986; Domingue et al., 1991).

In classical astronomy, photometry was used to compare the color and brightness of spatially unresolved objects and to seek temporal variations in these quantities on individual objects. With the advent of spacecraft observations, the uses of photometry were extended twofold. First, photometric modeling allowed the construction of quantitative maps of normal reflectance. In any given spacecraft image, most of the variation in intensity is due to the changing incident, and emergent angles of the radiation: by modeling the reflected radiation as a function of these changing viewing angles, the intrinsic changes in reflectance can be derived and mapped. A wide range of geophysical problems has been studied with such maps and the information they contain. For the icy Galilean satellites, such maps have been used to derive a quantitative distribution of frost deposits (Johnson et al., 1981); to understand the origin of dark-ray and dark-floor craters on Ganymede (Schenk and McKinnon, 1991); to accomplish photoclinometric studies (Squyres, 1981); to understand geologic processes (Buratti and Golombek, 1988); and to understand magnetospheric interactions with the surfaces (McEwen, 1986; Nelson et al., 1986; Sack et al., 1992).

The second new area of research enabled by spacecraft photometry is the derivation of disk-resolved physical parameters from the improved theoretical models. These models express the radiation reflected from the surface in terms of the following physical parameters: the single scattering albedo, the single particle phase function, the compaction properties of the optically active portion of the regolith, and the scale and extent of microscopically rough surface features. For the icy Galilean satellites, the results from these efforts have enhanced our understanding of magnetospheric and micrometeoritic

alteration processes (Buratti et al. , 1988; Buratti, 1991; Calvin and Clark, 1993; Domingue et al. 1991) and geologic histories (Helfenstein, 1986; Buratti and Golombek, 1988; Domingue and Hapke, 1992).

II. PHOTOMETRIC MODELS

For a cloud of particles with the single scattering albedo (w) low enough that multiple scattering can be neglected, the scattered intensity can be written (Chandrasekhar, 1960):

$$I(\mu, \mu_o, \alpha) = F \cdot P(\alpha) \frac{w}{4} \frac{\mu}{\mu + \mu_o} \quad (1)$$

where μ and μ are the cosines of the incidence (i) and emission (ϵ) angles (see Figure 01), a is the solar phase angle, πF is the plane parallel incident solar flux (at i=0°), and P(a) is the phase function of a single particle. The single scattering albedo is defined by

$$w = \frac{1}{4\pi} \int_{4\pi} P(\cos\theta)\, d\Omega \quad (2)$$

where O = a - 180° and dΩ is an element of solid angle. The phase function is a mathematical description of how the intensity of reflected light depends on the scattering direction. It is an indicator of the physical character of individual particles in the upper regolith, including their size and size distribution, shape, and optical constants. Small or transparent particles tend to be more isotropically scattering because photons survive to be multiply scattered; forward scattering occurs when photons exit particles in the direction away from the light source. One simple representation of the single particle phase function is the Henyey-Greenstein equation, originally used to describe dust particles in the interstellar medium (Henyey and Greenstein, 1941):

$$P(\cos\theta, g) = \frac{1 - g^2}{(1 + g^2 - 2g\cos\theta)^{3/2}} \quad (3)$$

where g = $\langle \cos\theta \rangle$ and ranges from -1, which is pure backscattering to g = +1, which is pure forward scattering (g = O is isotropic scattering). Double-lobed Henyey-Greenstein functions (Domingue et al. , 1991) have been utilized for Europa, while a second-order Legendre polynomial has been used to describe the single particle phase function of Ganymede (Helfenstein, 1986) .

It has been found repeatedly that eqt. (1) can be applied successfully to photometric observations of dark surfaces, including the Moon (Hapke, 1966), Mercury (Hapke, 1977), Mars and its moons (Noland, 1975), and Ganymede and

at small solar phase angles (. 120) are important for determining the compaction state of the regolith and observing coherent backscatter, whereas spacecraft observations are essential for determining the macroscopically rough nature of the surface.

For surfaces with normal reflectance greater than 0.6, multiple scattering can no longer be neglected in modeling the photometric properties of the surface (Buratti, 1984). The first celestial planetary surface for which eqt. (1) was shown to be inadequate was Europa (Buratti and Veverka, 1983). Although high albedo surfaces in the lab and fresh terrestrial snow scatter radiation approximately according to Lambert's law ($I \cdot F\mu_o$), the surface of Europa (and other planetary surfaces that are even brighter, such as Enceladus) cannot be described by this function. To adequately describe the contribution of multiply scattered photons, one might consider a semi-infinite layer of individual isotropically scattering particles. For this case, the reflected intensity is given by Chandrasekhar (1960):

$$I(\mu, \mu_o) = F\frac{w}{4}\frac{\mu}{\mu+\mu_o} H(\mu) H(\mu_o) \qquad (5)$$

where the H-functions are given in Table II of Chandrasekhar. For non-isotropic particles, an approximate extension of eqt. 5 is given by (Hapke, 1981, 1984, 1986; Goguen, 1981):

$$I(\mu, \mu_o, \alpha) = F\frac{w}{4}\frac{\mu_o}{\mu+\mu_o} S(\alpha) P(\alpha) + H(\mu) H(\mu_o) - 1) R(\mu, \mu_o, \alpha) \qquad (6)$$

where *S(a) is* a function describing the opposition effect, and $R(\mu,\mu_o,\alpha)$ is a function describing the effects of macroscopic roughness. This equation is derived under the assumption that radiation which is multiply scattered is isotropic. The effects of roughness, however, apply to both singly and multiply scattered photons (although current roughness models neglect the partial illumination of primary shadows by multiply scattered photons) .

A useful photometric function representing a combination of eqt. 1 (the so-called "Lommel-Seeliger" or lunar scattering law) and Lambert's law is given by

$$I(\mu, \mu_o, \alpha) = F(A\frac{\mu}{\mu+\mu_o}(\alpha) + (1-A)\mu_o) R(\mu, \mu_o, \alpha) \qquad (7)$$

where A is a term describing the fraction of light that is multiply scattered (A=1 corresponds to pure single scattering). In this interpretation, the singly scattered radiation is described by the first term, and the multiply scattered radiation is described by the second term. Although this equation cannot be

derived rigorously, Goguen (1981) has shown that it is a valid approximation to eqt. (6), except for extreme values of μ and μ_o. It has proven useful in describing the photometric properties of Europa (Buratti and Veverka, 1983) and the bright satellites of Saturn (Buratti and Veverka, 1984).

It is important to note that no planetary surface, even that of Enceladus with a geometric albedo of 1, approximates a Lambert. scatterer. *It is incorrect to model a planetary surface by Lambert's law for any application whatsoever.*

'I'he acquisition of spacecraft images has enabled extensive photometric modeling of disk-resolved planetary surfaces. Disk-integrated measurements (primarily Earth-based) continue to be useful because they offer constraints of fits to photometric models, and because they provide global descriptions of photometric properties. Furthermore , spacecraft images give only a snapshot in time, have limited spectral coverage, and are often restricted to specific viewing geometries (Voyager observations, for example, are lackingin observations at small solar phase angles). The primary disk integrated parameters are the disk-integrated brightness with respect to solar phase angle (from which the commonly quoted phase coefficient is derived), the disk integrated brightness with respect to orbital phase angle (from which longitudinal inhomogeneities in albedo and color can be observed), the geometric albedo , the phase integral, and the Bond albedo. The geometric albedo (p) is the ratio of the flux received from a reflecting body *at a solar phase angle of 0* to the flux expected by a perfectly diffusing disk of the same cross-sectional area in the same geometry. The phase integral, defined by

$$q=2\int_0^{\pi}\Phi(\alpha)\sin\alpha\, d\alpha \qquad (8)$$

where $\Phi(\alpha)$ is the disk-integrated brightness, describes the directional scattering properties of the object. 'l'he Bond albedo is defined by $A_B = p \cdot q$. A summary of the disk-int:egrat.ed properties of the icy Galilean satellites is listed in Table 1.

111, SUMMARY OF SURFACE PROPERTIES DERIVED FROM PHOTOMETRIC MODELS

In summary, the parameters to be fit to photometric observations of the icy Galilean satellites are: w, the single scattering albedo; g, the asymmetry factor expressing the average directional scattering properties of the particles; θ, the average slope angle of the surface; and the fraction of the optically active portion of the regolith occupied by particles. The last parameter depends on the particle size distribution, which is unknown for the icy Galilean satellites,

although reasonable assumptions can be made. Table II provides a summary of the surface properties derived from photometric models for the leading and trailing hemispheres of Europa, Ganynrede and Callisto.

A. Europa. Europa was the first Galilean satellite to be fit to a photometric model describing the surface in terms of physical parameters (Buratti, 1985). This early work showed that the surface properties of Europa were markedly different from those exhibited by other regoliths, both icy and rocky. Europa was shown to have a much more compacted surf-ace, a smaller slope angle (-230), and a more isotropic phase function than the Moon or the bright icy satellites of Saturn. Analysis of observations from the *International Ultraviolet Explorer (IUE)* satellite confirmed that Europa's surface is more compacted than the other Galilean satellites (Buratti et al. , 1988). The leading side of Europa was shown to lack an opposition surge and to be much more compact (~25% void space) than the trailing side (~79% void space), for which an opposition surge was observed. Later analysis of Europa's surface based on ground-based visible observations obtained by Lockwood and Thompson (1992) , including some at very small solar phase angles, showed that both the leading and trailing sides of Europa had very fluffy surfaces (~96% void space) similar to terrestrial powdery snow (Domingue et al. , 1991 ; see Table 11 and Figure 2). 'l'his interpretation assumed that the particle size distribution for Europa was similar to that of the Moon, and that the large opposition spike observed at $\alpha < 1°$ was due to the disappearance of mutual shadows cast among surficial particles. Another interpretation is that the surge is due to coherent backscatter of multiply scattered photons from Europa's surface (Hapke, 1990), in which case the surface of Europa could still be compacted (the exact relationship between surficial compaction and the width of an opposition surge due to coherent backscatter is not yet well-understood). A study of Europa's individual terrains showed that the only significant difference in their scattering properties was contained in the single scattering albedo (Domingue and Hapke, 1992). This difference was attributed to the addition of internal scatterers and associated darkening with increased exposure to magnetospheric ion bombardment . The other significant spatial difference for Europa's surface is an increased backscattered component in the single particle phase function for the leading hemisphere (Domingue et al. , 1991).

B. Ganymede. In the first analysis of Voyager images of Ganymede and Callisto, Squyres and Veverka (1981) showed that the surfaces of these two bodies scattered light according to eqt. (l). In the first analysis of these images in terms of the physical parameters entailed in eqt. (6), Helfenstein (1986) claimed that there existed significant differences in the average properties of Ganymede's two major terrains, the grooved terrain and the dark, cratered

terrain. Specifically, the cratered terrain was distinguished by: 1) a lower single scattering albedo; 2) a larger average tilt angle; 3) a more isotropic single particle phase function; and 4) a more compacted surface. The higher state of compaction for the cratered (presumably older) terrain suggested the development of dark lag deposits resulting from regolith devo].atization and ice welding of silicates. The less compacted nature of the brighter terrains suggested the growth of ice crystals at the surface. *IUE* observations suggested that the fraction of void space in Ganymede's regolith was '-83%, less than that of the other icy Galilean satellites (if one assumes that Europa's sharply peaked opposition surge is due to the effects of shadowing; see Section IV). An analysis of a combined data set of Voyager and ground-based measurements (Buratti, 1991) showed that there existedno differences between the leading and trailing hemispheres in surficial compaction, roughness, or the single particle phase function. In an application of photometric theory entailing a two-layer model, Hillier et al. (1994) produced a best-fit result showing that the polar caps of Ganymede consist of. relatively clean, thin (7 0.2, with a physical thickness of 1 mm or less), transparent frost with a single scattering albedo of '0.99 and a Henyey-Greenstein g=-0.33. The high single scattering albedo and thinness of the polar frost suggests that. they are the result of an ongoing deposition of sputtering products. This work also offered evidence that the roughness of the cratered terrain and the younger grooved terrain was not significantly different.

C. Callisto. Even before the Voyager encounter, telescopic observations of Callisto showed the leading side had a measurably larger opposition surge than the trailing side (Blanco and Catalano, 1974; Minis ancl Thompson, 1975). In an analysis combining both ground-based and Voyager observations, Buratti (1991) showed that not only was the upper regolith of the trailing side of Callisto more compacted, it scattered radiation more isotropically and was less rough (see Table II and Figure 3). This hemispheric dichotomy was explained in terms of enhanced micrometeoritic erosion on the leading side. An analysis of the spectrum of Callisto between 2.0 and 2.5 μm suggested that the surface of the trailing hemisphere contained larger ice grain sizes (Calvin and Clark, *1993),* which would be expected if micrometeoritic comminution processes were minimized on this hemisphere.

IV. SUMMARY AND DISCUSSION

Photometric models describing the physical properties of the optically active portion of planetary surfaces have been fit to the wealth of spacecraft observations obtained during the last 15 years. For the icy Galilean satellites these results have led to the derivation of surficial physical properties,

including the compaction state of the upper regolith, the roughness of the surface , and the single particle albedo and phase function. One general result is that some icy satellites, including Ganymede and Callisto, have regoliths with texture and roughness similar to that of the Moon, even though their surfaces consist mainly of water ice rather than rocky material. This similarity means that the erosional processes that determine the structural properties of regoliths (primarily meteoritic and magnetospheric bombardment) have comparable effects on icy and rocky bodies.

'I'he compaction states of the regoliths of the icy Galilean satellites show significant differences. In general, Callisto is the most. tenuous, with void spaces of '90%. This result is consistent with an increased exposure time to meteoritic bombardment on Callisto's primordial surface. Callisto's leading side is more compacted than the trailing side; again this difference can be attributed to enhanced micrometeoritic erosion. Europa's phase curve between 1° and 40° is very flat (Buratti and Veverka, 1983; Domingue et al. , 1991) , which suggests its regolith is extremely compacted. However, recent telescopic observations by Lockwood and Thompson (1992) reveal a sharply peaked opposition surge below 1°: if this effect is due to shadow hiding it would imply a very fluffy surface, with void space of ~96%. Given the overall flatness of Europa's phase curve, it is more likely that the surge is caused by an optical phenomenon such as coherent backscatter (Hapke, 1990).

In general, the single particle phase functions of the Galilean satellites are more backscattering than terrestrial ice and snow. Verbiscer et al, (1990) suggest that the ice itself - and not the opaque material - is backscattering, and that the way the ice is organized in conglomerations may be the key property. Both Callisto and Europa show measurable differences in this parameter for their leading and trailing hemispheres , The leading hemispheres are more backscattering for both bodies; in both cases the difference can be attributed to enhanced meteoritic erosion on the leading side.

Of the Galilean satellites, Europa has the smoothest surface, with mean slope angles of only '10 degrees (Buratti, 1985; Domingue et al.. , 1991, Domingue and Hapke, 1992). Because photometric modeling "sees" surface facets smaller than the spatial resolution of the detector, this result means Europa is smooth down to the smallest features, which are represented by clumps of particles. The highest resolution Voyager images show minimal topography at scales of a few kilometers; the highest features (the scalloped ridges) are only a few hundred meters (Lucchitta and Soderblom, 1982) . All these lines of evidence point to a recent resurfacing event on Europa. The mean slope angle for Ganymede and Callisto is about *'30* degrees, similar to that of the Moon (Helfenstein, 1986;

Buratti, 1991). Significant spatial differences exist: Helfenstein (1986) found that Ganymede's dark cratered terrain was rougher than the grooved terrain, and Buratti (1991) showed that the leading side of Callisto was rougher than the trailing side, again perhaps as the result of enhanced meteoritic erosion,

Two major concerns involving photometric modeling exist: the uniqueness of the solutions, and their similarity to the actual physical conditions of the surface. The degree of uniqueness is primarily a matter of obtaining observations over a full range of viewing geometries, Helfenstein et al. (1988) identified specific ranges of geometries over which the first derivative of the various parameters changes rapidly: it is observations in these ranges that are crucial *to* attaining uniqueness. Buratti (1985; 1991) and Domingue et al., *(1991)* showed that disk- integrated observations , when combined with disk resolved measurements , can eliminate certain sets of solutions.

Because of the many simplifying assumptions that have gone into the models, the results may not be physically real. These assumptions include spherical particles, simple particle phase functions, and ideally shaped rough features. In a more exact radiative transfer calculation of the single particle phase function, Mishchenko (1994) has shown that the phase functions of planetary surfaces may in fact be forward scattering. On the other hand, Goguen (1993) has shown that if one relaxes the assumption of isotropy for multiply scattered photons, the backward scattered intensity *increases .* Undoubtedly, more physically realistic descriptions of planetary surfaces will emerge as efforts at theoretical modeling progress. At this time, it is most useful if one thinks of the parameters listed in Table II as *model* parameters revealing similarities and differences in the structure of planetary surfaces.

ACKNOWLEDGEMENTS

I thank Deborah Domingue and Paul Helfenstein for providing detailed reviews . This work was performed at the Jet Propulsion Laboratory, California Institute of l'ethnology, under contract with the National Aeronautics and Space Administration.

REFERENCES

Arvidson, R. E , E. A. Guinness, M. A. Dale-Bannister, J. Adams, M. Smith, p. R. Christensen, R. B. Singer 1989. Nature and distribution of surficial deposits on Chryse Planitia and vicinity, Mars. *J.Geophys.Res.* 94, 1573-1587.

Blanco, C., and S. Catalano 1974. On the photometric variations of the Saturn and Jupiter satellites. *Astron.Astrophys.*33,105-111.

Buratti, B. J. 1984. Voyager disk resolved photometry of the Saturnian satellites. *Icarus 59, 392-405.*

Buratti, B. J., and J. Veverka 1983. Voyager photometry of Europa. *Icarus 55,* 93-110.

Buratti, B. J., and J. Veverka 1984. Voyager photometry of Rhea, Dione, Tethys, Enceladus, and Mimas. *Icarus 58, 254-2'64.*

Buratti , B. J., and J. Veverka 1985. Photometry of rough planetary surfaces: the role of multiple scattering. *Icarus 64, 320-328.*

Buratti, B. J. 1985, Application of a radiative transfer model to bright icy satellites. *Icarus 61,* 208-217.

Buratti, B. J. 1991. Ganymede and Callisto: Surface textural dichotomies and photometric analysis. *Icarus 92, 312-323.*

Buratti, B. J, and M, Golombek 1988. Europa: Geologic implications of spectrophotometry *Icarus* 75, 437-449.

Buratti, B. J., Nelson. R. M., and A. L. Lane 1988. Surficial textures of the Galilean satellites. *Nature 333, 148-151.*

Calvin, W. M., and R. N. Clark 1993. Spectral distinctions between the leading and trailing hemispheres of Callisto: New observations. *Icarus 104, 69-78.*

Chandrasekhar, S. 1960. *Radiative Transfer,* Dover, New York.

Domingue, D. L. , and B. W. Hapke 1992. Disk-resolved analysis of Europan terrains. *Icarus* 99, 70-81.

Domingue, D. L. , B. W. Hapke, G. W. Lockwood and D. T. Thompson 1991. Europa's phase curve: Implications for surface structure. *Icarus 90, 30-42.*

Goguen, J.D. 1981. A theoretical and experimental investigation of the photometric functions of particulate surfaces. PhD Thesis, Cornell University, Ithaca, NY.

Goguen, J. D., A quantitative test of the applicability of independent scattering to high albedo planetary regoliths. Submitted to *Icarus,* 1993.

Hapke, B. 1966. An improved lunar theoretical photometric function. *Astron. J. 71, 333-339.*

Hapke, B. 1977. Interpretations of optical observations of Mercury and the moon. *Phys . Earth Planet. Inter. 1.5, 264-274.*

Hapke, B. 1981. Bidirectional reflectance spectroscopy. 1. Theory *J. Geophys. Res. 86, 3039-3054.*

Hapke, B. 1984, Bidirectional reflectance spectroscopy. 3. Correction for macroscopic roughness. ***Icarus 59, 41-59.***

Hapke, B. 1986. Bidirectional reflectance spectroscopy. 4. The extinction coefficient and the opposition effect. *Icarus 67, 264-?.80.*

Hapke, B. 1990. Coherent backscatter and the radar characteristics of outer planet satellites. *Icarus 88, 407-417.*

Helfenstein, P. 1986. Derivation and analysis of geological constraints on the

emplacement and evolution of terrains on Ganymede from differential photometry, PhD Thesis, Brown University, Providence, RI.

Helfenstein, P. , J. Veverka, and P. Thomas 1988. Uranus satellites: Hapke parameters from Voyager disk integrated photometry. *Icarus 74, 231-239.*

Henyey, L. G., and J. Greenstein 1941. Diffuse radiation in the Galaxy. *Astrophys. J. 93, 70-83.*

Hillier, J., P. Helfenstein. , A. Verbiscer, J. Veverka, R. H. Brown, J, Goguen, and T. V. Johnson 1990. Voyager disk-integrated photometry of Triton. *Science 250, 419-421.*

Hillier, J., P. Helfenstein, and J. Veverka, 1994. Ganymede polar caps: the thickness from photometry. Icy Galilean Satellites Conference, San Juan Capistrano, CA, Feb. 1-3, 1994. p. 35-36 of abstract book.

Irvine , W. M. 1966. The shadowing effect in diffuse radiation. *J. Geophys. Res.* 71, 2931-2937.

Johnson, T, V., L. A. Soderblom, J, A. Mosher, G. H. Danielson, A. F. Cook, and P. Kupferman 1983. *J. Geophys. Res.* 88, 5789-5805.

Thompson, D.T., and G. W. Lockwood 1992. Photoelectric photometry of Europa and Callisto 1976-1991. *J. Geophys. Res.* 97, 14,761-14,771.

Lucchitta, B., and L. Soderblom 1982. The geology of Europa, in *Satellites of Jupiter* (D, Morrison, cd., University of Arizona Press, Tucson), 521-555.

Lumme, K. and E. Bowell 1981., Radiative transfer in the surfaces of atmosphereless bodies. *Astron. J. 86, 1694-1704,*

Minis, R. L., and D. T. Thompson 1975. UBV photometry of the Galilean satellites. Icarus 44, 408-419.

Mishchenko, M. I. 1994. Asymmetry parameters of the phase function for densely packed scattering grains, *J. Quant. Spectrosc. Rad. Transfer 52, 1994.*

McEwen, A. 1986. Exogenic and endogenic albedo and color patterns on Europa. *J. Geophys. Res. 91, 8077-8097.*

Nelson, M. L., T. B. McCord, R. N. Clark, T. V. Johnson, D. L. Matson. J. A. Mosher , and L. A. Soderblom 1986. Europa: Characterization and interpretation of global spectral surface units. *Icarus 65, 129-151.*

Noland, M. 1975, Photometric properties of the satellites of Mars and Saturn. PhD thesis , Cornell University, Ithaca, NY

Sack, N. J., R. E. Johnson, J, W. Boring, and R. A. Baragiola 1992. The effect of magnetospheric ion bombardment on the reflectance of Europa's surface. *Icarus* 100, 534-540,

Schenk, P. and W. McKinnon 1991. Dark-ray and dark-floor craters on Ganymede, and the provenance of large impactors in the Jovian system. *Icarus 89, 318-346.*

Schoenberg, E. 1925. Untersuchungen zur Theorie der Beleuchtung des Mondes auf Grund photometrischer Messungen. *Acts Sot. Sci. Fenn. 9, 6-71.*

Seeliger, H. 1887. Zur theorie beleuchtung der grossen planeten insbesondere des

Saturn, *Abhandl. Bayer. Akad. Wiss. Math.-Naturw. Kl.* 16, 405-516

Squyres, s. ,1981. The morphology and evolution of Ganymede and Callisto. PhD Thesis , Cornell University, Ithaca, NY.

Squyres, S. and J. Veverka 1981. Voyager photometry of surface features on Ganymede amd Callisto. *Icarus 46, 137-155*

Verbiscer, A., P. Helfenstein, and J. Veverka 1990. Backscattering from frost on icy satellites in the outer Solar System. *Nature 347, 162-164.*

TABLE I - HEMISPHERIC DISK-INTEGRATED PHOTOMETRIC PROPERTIES OF THE ICY GALILEAN SATELLITES (0.47 μm)

Satellite	Geometric albedo	Phase integral	Bond albedo	Source
Europa (L)	0.92			(1)
Europa (T)	0.71			"
Europa (integral)		1.09 ± 0.11	*0.62 ± 0.14*	(2)
Ganymede (L)	0.46 ± 0.05			(3)
Ganymede (T)	0.43 ± 0.05			"
Ganymede (integral)		0.78 ± 0.06	0.35 i 0.03	"
Callisto (L)	0.23 ± 0.02			(3)
Callisto (T)	0.20 ± 0.02			"
Callisto (integral)		0.51 ± 0.06	0.11 i 0.02	"

L-=Leading hemisphere; T--trailing hemisphere
(1) Domingue et al., 1991
(2) Buratti and Veverka, 1983
(3) Buratti, 1991

TABLE II - SUMMARY OF PHOTOMETRIC SURFACE PROPERTIES OF THE ICY GALILEAN SATELLITES (0.47 μm)

Satellite	Single scattering albedo (w)	Slope angle e (degrees)	g	% void space	Source
Europa (L)	0.92	10	-0.43; 0.079¶	96	(1)
Europa (T)	0.90	10	-0.43; 0.287¶	96	"
Ganymede (L)	0.82 ± 0.03		-0,20 i 0,04	80	(2)
Ganymede (T)	0.78 ± 0.03	29 ± 2	-0.21 ± 0.04	80	"
Callisto (L)	0,43 ± 0.03	36 ± 3	-0.23 i 0.02	92	(2)
Callisto (T)	0,45 ± 0.03	2 9 * 3	-0.17 i 0.02	88	"

¶Two-component Henyey-Greenstein phase function
(1) Domingue et al., 1991
(2) Buratti, 1991

FIGURE CAPTIONS

1. Photometric geometry on a sphere, showing the following angles: the radiance incident (i) and emission (ϵ) angles, the solar phase angle ***(a)***, and the photometric latitude (ψ) and longitude (ω).

2. Voyager and telescopic observations of the trailing hemisphere of Europa, with the model fits from Table II (based on Figure 7B from Domingue et al., 1991).

3. Voyager and telescopic observations of the leading and trailing hemispheres of Callisto, with the model fits from Table II (Buratti, 1991).

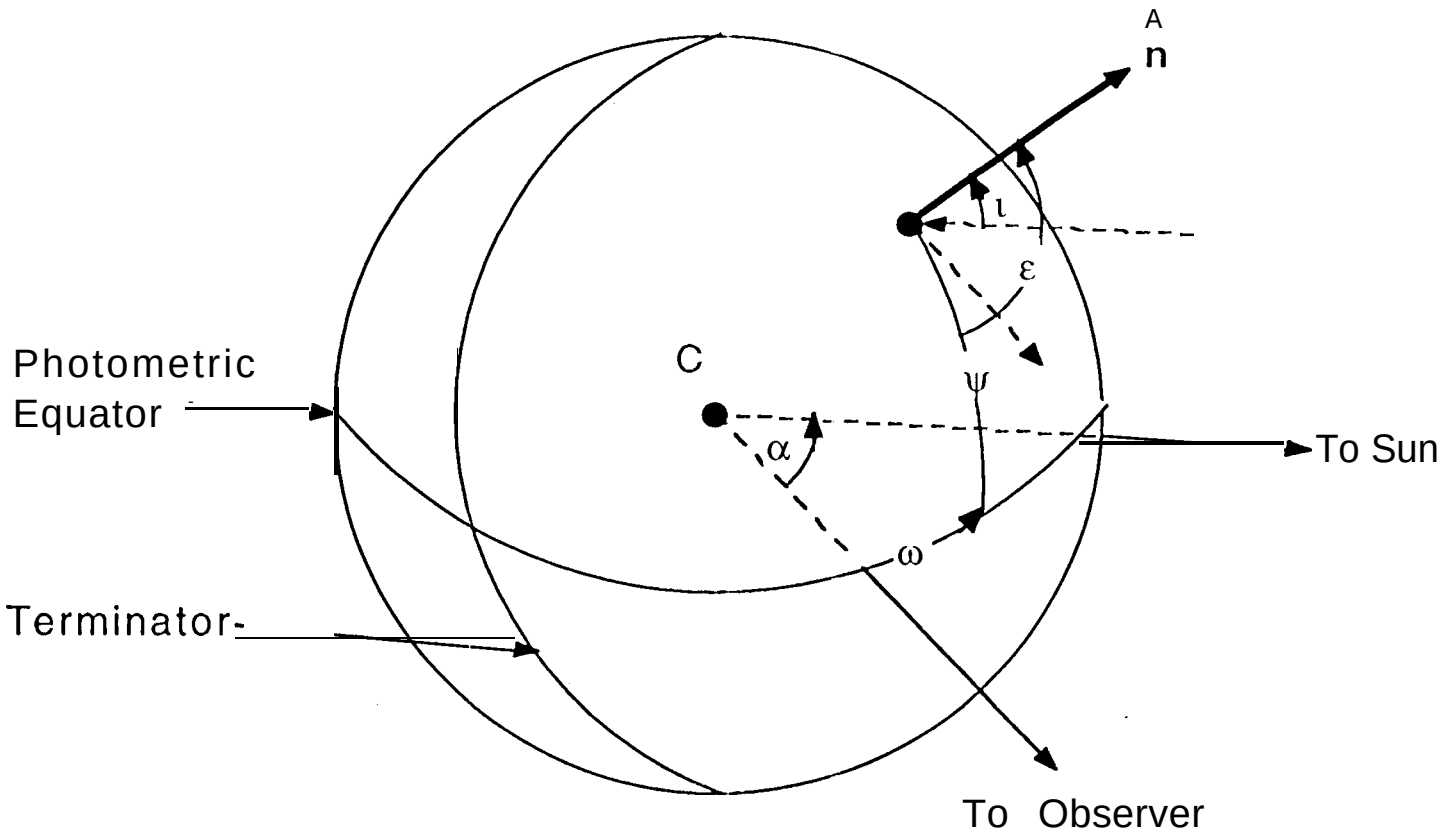
A
n
ι
ε
C
ψ
α
ω
Photometric
Equator
To Sun
Terminator
To Observer

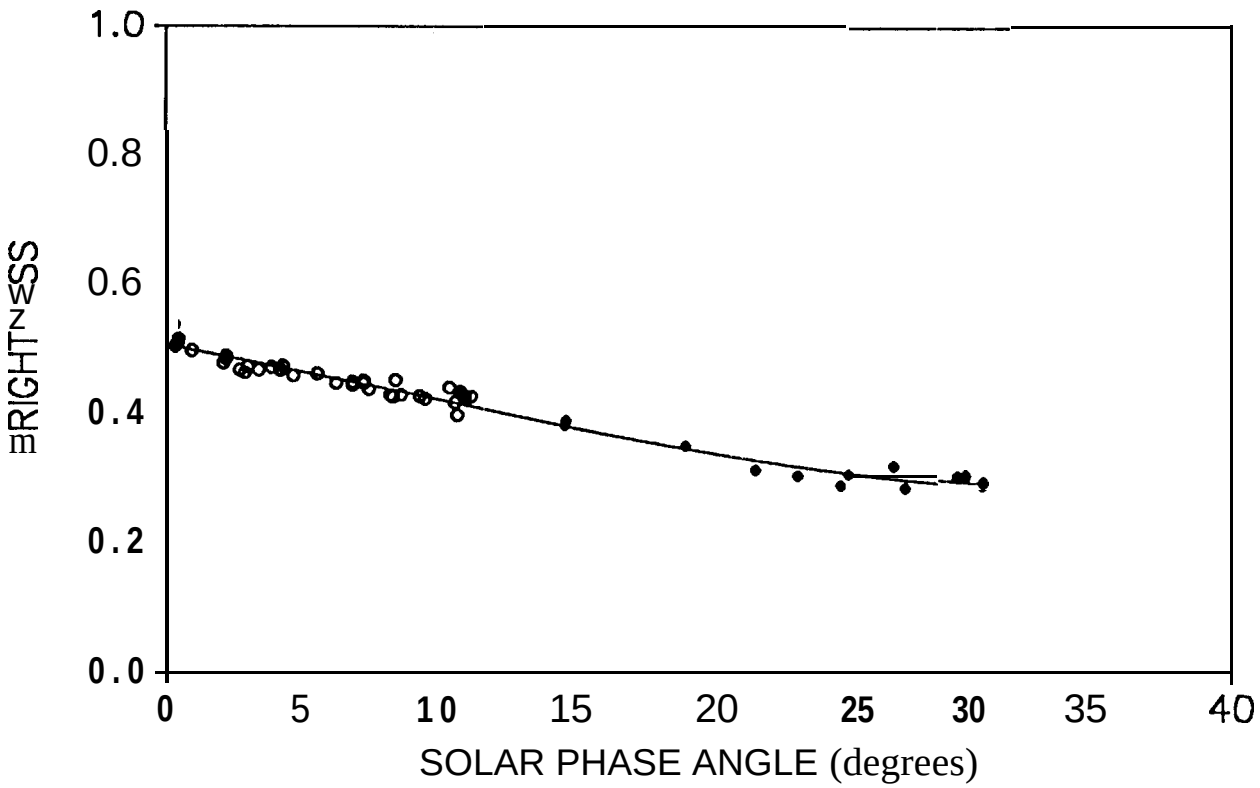
1.0
0.8
0.6
0.4
0.2
0.0
BRIGHTNESS
0
5
10
15
20
25
30
35
40
SOLAR PHASE ANGLE (degrees)

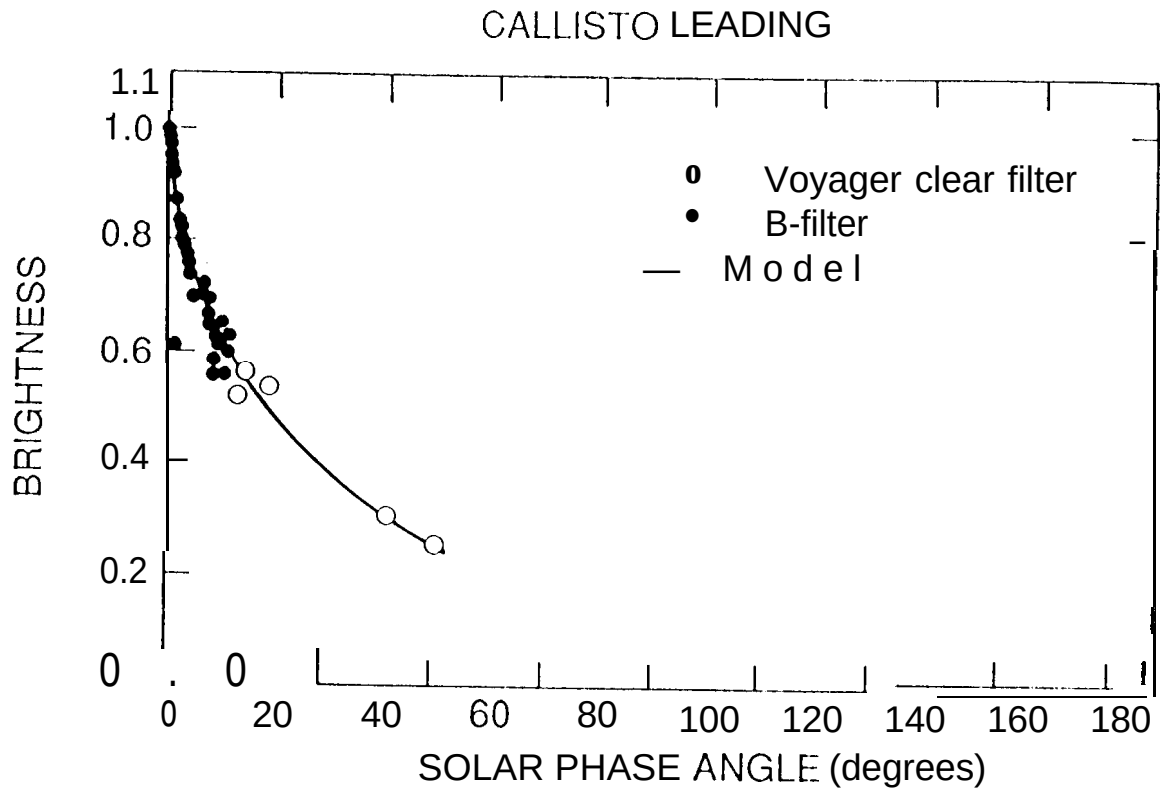
CALLISTO LEADING
BRIGHTNESS
1.1
1.0
0.8
0.6
0.4
0.2
0
0
20
40
60
80
100
120
140
160
180
SOLAR PHASE ANGLE (degrees)
Voyager clear filter
B-filter
Model

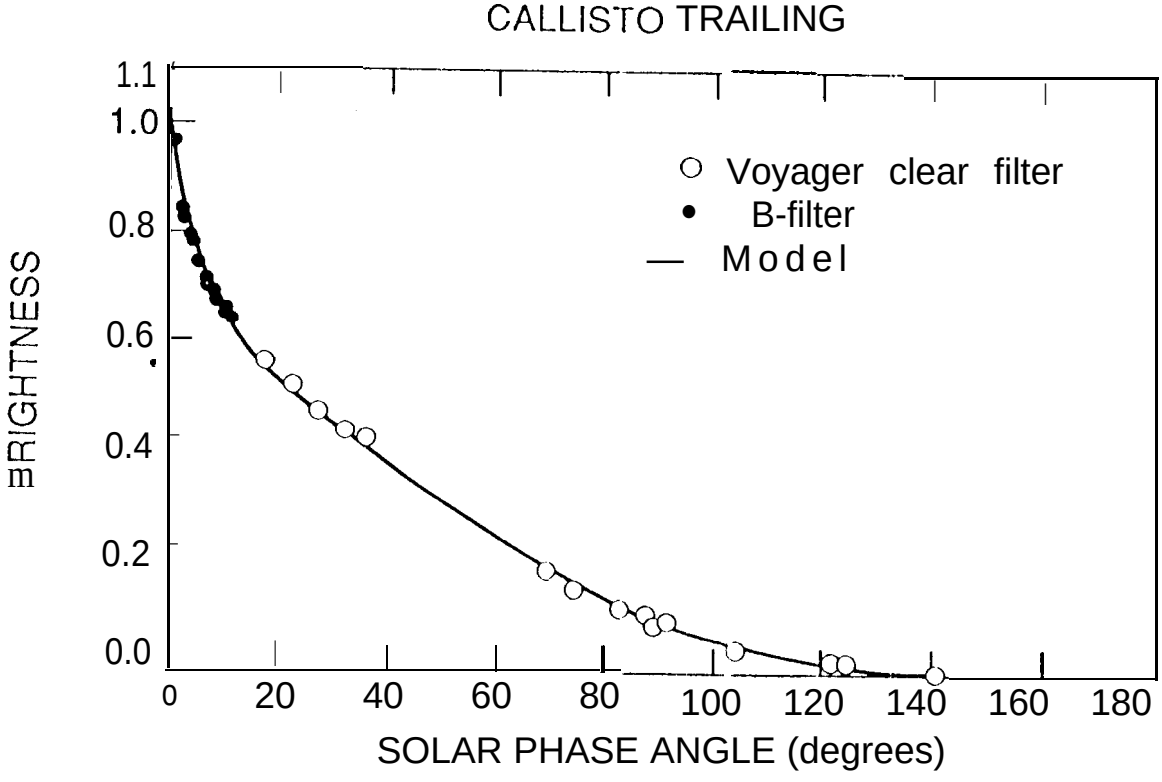
CALLISTO TRAILING
BRIGHTNESS
1.1
1.0
0.8
0.6
0.4
0.2
0.0
0
20
40
60
80
100
120
140
160
180
SOLAR PHASE ANGLE (degrees)
Voyager clear filter
B-filter
Model